SiliconPV 2023, 13th International Conference on Crystalline Silicon Photovoltaics
Si-Based Tandem Cells in Combination With Perovskites, III-V and Alternative Materials
https://doi.org/10.52825/siliconpv.v1i.878

Published: 22 Feb. 2024

Both-Sided TOPCon Solar Cells – Towards a Lean Process Flow for Silicon Bottom Solar Cells

Johannes Seif[1][https://orcid.org/0000-0003-1230-8099], Jana-Isabelle Polzin[1][https://orcid.org/0000-0002-2372-164X], Mathias Bories[1][https://orcid.org/0000-0002-4960-4062], Martin Hermle[1][https://orcid.org/0000-0002-2412-1734], and Martin Bivour[1]

[1]Fraunhofer-Institute for Solar Energy Systems ISE, Germany

Abstract. Silicon solar cells with both-side full-area passivating hole and electron contacts are viable candidates for application as bottom cells in tandem architectures. In this contribution, cells with poly-Si based contacts at both sides are investigated as a potential upgrade to the emerging i-TOPCon single junction devices featuring a passivating contact (poly-Si(n)/SiO_x) only at the rear side and an alternative to the SHJ technology featuring a-Si based full-area passivating hole and electron contacts. We show that a higher thermal budget is needed to mediate between poly-Si(p)/SiO_x hole and poly-Si(n)/SiO_x electron contact when the same thermal interfacial SiO_x is applied. This is addressed by using a PECVD oxide that is adapted to the needs of the hole and/or the electron contact. We present a proof-of-concept poly-Si(n)/SiO_x/c-Si/SiO_x/poly-Si(n) device with emphasis on a lean process flow. An all-PECVD process sequence for the hole contact, i.e., plasma oxides+i/p-a-Si deposited at 200°C in the same chamber was applied. With co-annealing of the contacts, no additional hydrogenation, and no edge insulation step, we observe no shunting and obtain efficiencies of up to 20.8% for M2 size cells, so far.

Keywords: Silicon Bottom Cells, TOPCon, Tandem Solar Cells

1. Introduction

Recent developments of tandem devices have shown that it is possible to overcome the fundamental limit of Silicon single-junction devices. Power conversion efficiencies of up to 35.9% have been demonstrated in two-terminal tandem devices based on a TOPCon² like bottom cell and a III/V top cell [1]. For the c-Si/perovskite tandem structures, the current world record reaches efficiencies above 32% [2], which, relies on silicon heterojunctions as bottom cell.

In our contribution, we report on the learnings gained from the TOPCon single junction and TOPCon/III-V tandem development and their future transfer towards TOPCon/perovskite devices with a lean process sequence and potential to integrate a Silicon-based tunneljunction (TJ) [3]. The focus here is on the different nature of n-type and p-type TOPCon electron and hole contacts and the resulting design trade-off with respect to passivation and transport losses in TOPCon² solar cells. We showcase that an increased freedom of design results from “asymmetric” oxide properties at the hole and electron contact that enables a single co-annealing step for activating both the n-TOPCon and p-TOPCon.

2. Experimental Approach

Firstly, the properties of n- and p-type TOPCon structures are investigated with regards to their passivation quality and contact resistivity (ρ_c) by means of symmetric lifetime samples. Subsequently, the optimized layer stacks are implemented into full-area, both-sided TOPCon solar cells.

2.1 Lifetime Test Structures

Symmetric test structures were first fabricated using 1 Ωcm n- or p-type 4-inch FZ wafers with a thickness of 200 or 250 µm, respectively. The wafers were either thermally oxidized (TO) in O_2/N_2 gas or oxidized by a nitrous oxide plasma (PO) in the same chamber used for doped a-Si deposition. Here, a 13.56 MHz parallel plate PECVD reactor was used with PH_3 or TMB as doping gases. The annealing temperature (T_{ann}) for poly-Si formation was applied in the range of 850–1000°C. Finally, the samples received a hydrogenation step using AlO_x and FGA annealing. The contact resistivity ρ_c across the poly-Si/SiO_x/c-Si contact was obtained using vertical *I-V* measurements.

2.2 Solar Cell Processing

In a second step, M2-sized devices were fabricated using single-side textured n-type Cz wafers. The interfacial oxide was grown thermally on both sides of the wafers (“TO + PECVD”) but for half of the solar cells the oxide at the p-type TOPCon rear side was substituted by the novel developed nitrous plasma oxide described above (“all PECVD p-TOPCon”). Doped a-Si layers were deposited with a thickness of 30 nm. A co-annealing step at 900°C for 10 min in N_2 atmosphere was performed to crystallize the full-area n-type a-Si(n) layer at the textured front and p-type a-Si(p) layer at the planar rear side. Cells were then finalized with both side TCO deposition of ITO:H and screen printing of a low-temperature silver paste. Note that the cells did not receive any additional hydrogenation step and edge insulation was done only by masking of the rear side TCO, i.e., no extra removal of poly-Si at the edges. Basically, the same back-end processing was applied as for our SHJ baseline, which leaves room for improvements to this TOPCon based cell architecture, i.e. TOPCon² cell design. Finally, the I-V data of the cells were measured at different subsequent post-processing curing steps in the range of 250 – 450°C. A schematic of the TOPCon² solar cell using an n-type Cz absorber and a process flow is depicted in Figure 1.

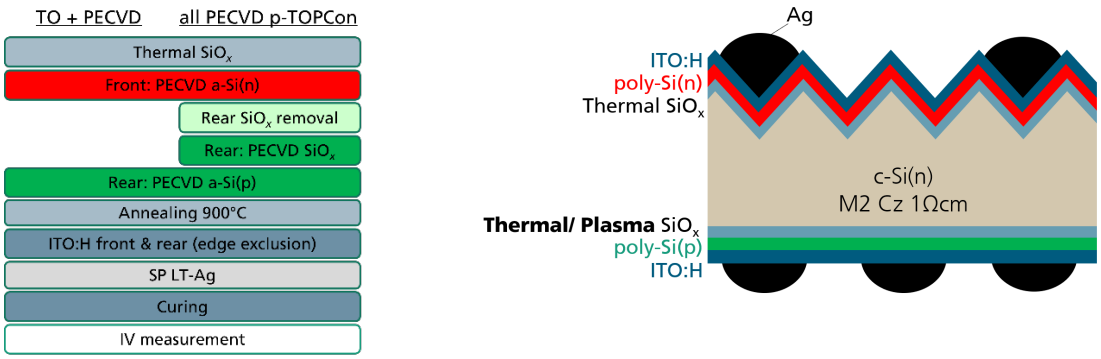

Figure 1. Process flow (left) and schematic (right) of both-sided n-type TOPCon² solar cell.

3. Advantage of Plasma Oxides for TOPCon Processing

The results obtained for symmetrical poly-Si(p) and poly-Si(n) structures from QSSPC and contact resistivity measurements are compiled in Figure 2.

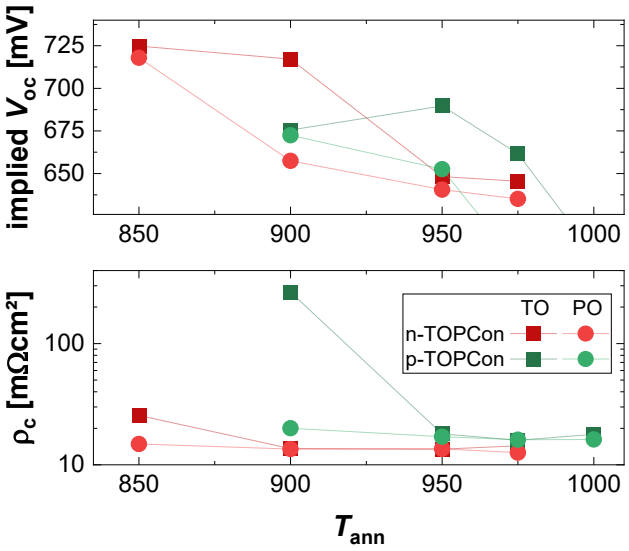

Figure 2. Surface passivation after hydrogenation (upper graph) and contact resistance (lower graph) for p- and n-TOPCon prepared with a thermally grown or plasma oxide derived from symmetrical test structures using different T_{ann} and interfacial oxides.

First, our results clearly show the discrepancy between n-type and p-type TOPCon contacts, where n-type provide better passivation (approx. 730 mV) while their p-type counterparts reach a lower level in the current development stage (approx. 700 mV). What is also apparent is that the TO/n-poly combination cannot sustain T_{ann} > 900°C with regards to iV_{oc}. For the TO/p-poly counterparts on the other hand higher temperatures of 950°C are needed for sufficiently low contact resistivities. It is evident that for the implementation into cells, a trade-off between passivation and contact resistivity must be found, which also defines the optimal co-annealing temperature for both doping types. Taking a closer look at the data obtained for TOPCon structures featuring a nitrous plasma oxide PO. n-type TOPCon only perform well at 850°C, the lowest T_{ann} tested here. At higher temperatures, the passivation breaks down. For PO/poly-Si(p), the situation is quite different. At 900°C the PO/poly-Si(p) contact performs almost equally well as the TO/poly-Si(p) contact in terms of passivation. But the PO/poly-Si(p) contact exhibits an acceptable resistivity of only 20 mΩ.cm^2 compared to the 300 mΩ.cm² obtained with a TO. As a showcase for the increased freedom of design for the use of such asymmetric oxide properties at the hole and electron contact, we chose to implement the PO/poly-Si(p)and TO/poly-Si(n) contacts in our proof-of-concept cells and co-annealed at 900°C. Please note that it is in principle possible to find well-working plasma oxidation processes for both contacts and likely reach voltages clearly above 700 mV as already shown in literature [4–6].

4. Both-Sided TOPCon Solar Cells

I-V results of TOPCon² cells with either TO on both sides or TO/poly-Si(n) at the front and PO/poly-Si(p) at the rear are shown in Figure 3(a)-(f).

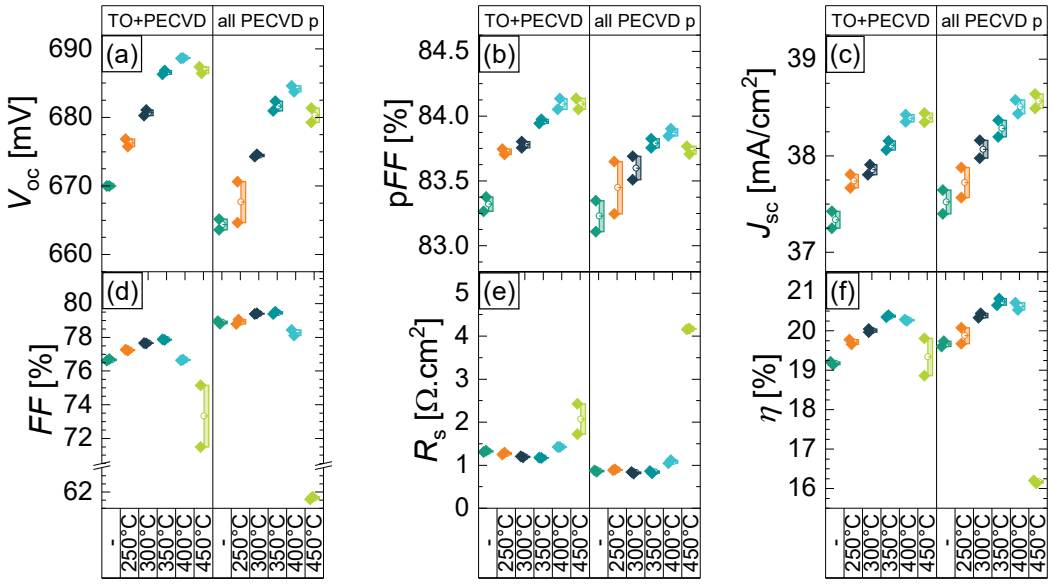

Figure 3. a) – f). I-V results for both-sided M2 TOPCon solar cells in the initial state, after annealing at 10 min at 250°C, 5 min at 300°C, 350°C, 400°C, and 450°C.

In the initial state, the cells reveal a low V_{oc} of max. 670 mV limited by e.g. the sputter damage during TCO deposition (Figure 3 a). This is found in samples with thermal (left) and all PECVD p-TOPCon rear side (right side). Nonetheless, improved passivation is reflected in the steady improvement in V_{oc} (as well as p*FF*) for annealing at up to 400°C due to curing of sputter damage and likely due to migrating atomic hydrogen from ITO:H to TOPCon for interface passivation [7]. The V_{oc} was slightly higher in the both side thermal oxide reference samples compared to those with plasma oxide at the rear side p-TOPCon. Furthermore, the J_{sc} increase up to 450°C annealing is dominated by an improved blue-response (QE not shown here) that may be linked to improved passivation at the poly-Si(n)/SiO_x/c-Si front surface field and a phase change of the ITO:H towards more crystalline material [8]. After reaching a curing temperature of 350°C, the *FF* drops due to an increase in R_s while the *pFF* keeps improving. A reasonable explanation for this trade-off between passivation and transport losses might be a parasitic oxide layer formed at the poly-Si/ITO interface [9] during the final annealing. Comparing the two test structures, the *FF* is higher (R_s is lower) in solar cells with a plasma oxide for p-TOPCon. This can be ascribed to the lower contact resistance of all-PECVD p-TOPCon presented for the test structures above. Finally, this is also reflected in the higher efficiency obtained for the cells with an all-PECVD hole contact with a maximum of 20.8%. Compared to the initial state, a gain of up to 1.5% absolute in efficiency is achieved after annealing at 350°C.

PECVD is considered a single-sided deposition technique, but it is usually accompanied by parasitic wrap-around of the doped a-Si layers potentially leading to shunts. Please note that no a-Si or poly-Si wrap-around removal step was performed for our cells. Therefore, it is important to note that despite this, we do not see any significant shunting of the cells, which exhibited shunt resistances of more than 4 kΩ.cm² (unaffected by curing).

5. Conclusion

In summary, we addressed different aspects that need to be considered when implementing both-sided TOPCon bottom cells for example as bottom cells in Perovskite-tandem devices. With regards to a lean process flow we showed that plasma oxidation can provide a good passivation and low contact resistivity which allows for a co-annealing step for the formation

of the n-TOPCon front and p-TOPCon rear contact. Based on this, we were able to realize full-area M2 TOPCon² solar cells with an efficiency of up to 20.8%. For the passivation of thin TOPCon layers no additional hydrogen source such as AlO_x/SiN_x dielectric capping layers were employed but the curing of the sputter damage is vital. More work is needed to understand the good shunting behavior found without any PECVD poly-Si wrap-around removal step.

Data availability statement

The data supporting the results of this contribution are available upon reasonable request from the corresponding author

Author contributions

Johannes Seif: Conceptualization, Data curation, Investigation, Visualization, Roles/Writing – original draft; Jana-Isabelle Polzin: Conceptualization, Visualization, Roles/Writing – original draft, Mathias Bories: Investigation, Martin Hermle: Funding acquisition – review & editing. , Martin Bivour: Conceptualization, Supervision, Writing – review & editing.

Competing interests

The authors declare no competing interests.

Funding

This work was supported by the German Federal Ministry for Economic Affairs and Energy BMWI within the research project “PaSoDoble” under contract no. 03EE1031A.

Acknowledgement

The authors would like to thank A. Leimenstoll, F. Schätzle, K. Zimmermann, S. Pingel and I. Koc for sample preparation and characterization.

References

1. P. Schygulla, R. Müller, D. Lackner, O. Höhn, H. Hauser, B. Bläsi, F. Predan, J. Benick, M. Hermle, S. W. Glunz, and F. Dimroth, Prog Photovolt Res Appl **30**, 869 (2022). DOI: https://doi.org/10.1002/pip.3503.
2. NREL, *Best Research-Cell Efficiency Chart*, <https://www.nrel.gov/pv/cell-efficiency.html>.
3. C. Luderer, M. Penn, C. Reichel, F. Feldmann, J. C. Goldschmidt, S. Richter, A. Hahnel, V. Naumann, M. Bivour, and M. Hermle, IEEE J. Photovoltaics **11**, 1395 (2021). DOI: https://doi.org/10.1109/jphotov.2021.3101177.
4. S. W. Glunz, B. Steinhauser, J.-I. Polzin, C. Luderer, B. Grübel, T. Niewelt, A. M. O. M. Okasha, M. Bories, H. Nagel, K. Krieg, F. Feldmann, A. Richter, M. Bivour, and M. Hermle, Prog Photovolt Res Appl (2021). DOI: https://doi.org/10.1002/pip.3522.
5. Y. Huang, M. Liao, Z. Wang, X. Guo, C. Jiang, Q. Yang, Z. Yuan, D. Huang, J. Yang, X. Zhang, Q. Wang, H. Jin, M. Al-Jassim, C. Shou, Y. Zeng, B. Yan, and J. Ye, Solar Energy Materials and Solar Cells **208**, 110389 (2020). DOI: https://doi.org/10.1016/j.solmat.2019.110389.

6. M. Stöhr, J. Aprojanz, R. Brendel, and T. Dullweber, ACS Appl. Energy Mater. **4**, 4646 (2021). DOI: https://doi.org/10.1021/acsaem.1c00265.

7. L. Tutsch, F. Feldmann, B. Macco, M. Bivour, E. Kessels, and M. Hermle, IEEE J. Photovoltaics, 10 (2020). DOI: https://doi.org/10.1109/jphotov.2020.2992348.

8. N. Juneja, L. Tutsch, F. Feldmann, A. Fischer, M. Bivour, A. Moldovan, and M. Hermle, “Effect of hydrogen addition on bulk properties of sputtered indium tin oxide thin films,” in *15th International Conference on Concentrator Photovoltaic Systems (CPV-15)* (AIP Publishing, 2019), p. 40008.

9. L. Tutsch, F. Feldmann, J. Polzin, C. Luderer, M. Bivour, A. Moldovan, J. Rentsch, and M. Hermle, Solar Energy Materials and Solar Cells **200**, 109960 (2019). DOI: https://doi.org/10.1016/j.solmat.2019.109960.